



UNIVERSITY OF LEEDS

This is a repository copy of *Mechanistic Understanding of Competitive Destabilization of Carbamazepine Cocrystals under Solvent Free Conditions*.

White Rose Research Online URL for this paper:

<https://eprints.whiterose.ac.uk/167284/>

Version: Accepted Version

Article:

Alsirawan, MHDB, Lai, X, Prohens, R et al. (5 more authors) (2020) Mechanistic Understanding of Competitive Destabilization of Carbamazepine Cocrystals under Solvent Free Conditions. *Crystal Growth & Design*, 20 (9). pp. 6024-6029. ISSN 1528-7483

<https://doi.org/10.1021/acs.cgd.0c00735>

© 2020 American Chemical Society. This is an author-accepted version of an article published in *Crystal Growth & Design*. Uploaded in accordance with the publisher's self-archiving policy.

Reuse

Items deposited in White Rose Research Online are protected by copyright, with all rights reserved unless indicated otherwise. They may be downloaded and/or printed for private study, or other acts as permitted by national copyright laws. The publisher or other rights holders may allow further reproduction and re-use of the full text version. This is indicated by the licence information on the White Rose Research Online record for the item.

Takedown

If you consider content in White Rose Research Online to be in breach of UK law, please notify us by emailing eprints@whiterose.ac.uk including the URL of the record and the reason for the withdrawal request.



eprints@whiterose.ac.uk
<https://eprints.whiterose.ac.uk/>

This document is confidential and is proprietary to the American Chemical Society and its authors. Do not copy or disclose without written permission. If you have received this item in error, notify the sender and delete all copies.

Mechanistic Understanding of Competitive Destabilization of Carbamazepine Cocrystals under Solvent Free Conditions

Journal:	<i>Crystal Growth & Design</i>
Manuscript ID	cg-2020-00735d.R1
Manuscript Type:	Article
Date Submitted by the Author:	n/a
Complete List of Authors:	Alsirawan, MHD Bashir; University of Bradford Faculty of Life Sciences, Center for Pharmaceutical Engineering Science Lai, Xiaojun; University of Leeds, School of Chemical and Process Engineering Prohens, Rafel; Universitat de Barcelona, Unitat de Polimorfisme i Calorimetria Vangala, Venu; University of Bradford, Centre for Pharmaceutical Engineering Science, School of Pharmacy and Medical Sciences Shelley, Petroc; The University of Manchester, School of Earth and Environmental Sciences Bannan, Thomas; University of Manchester, School of Earth, Atmospheric and Environmental Science Topping, David; University of Manchester, School of Earth, Atmospheric and Environmental Science Paradkar, Anant; Institute of Pharmaceutical Innovation, University of Bradford

SCHOLARONE™
Manuscripts

1
2
3
4
5
6
7
8
9
10
11
12
13
14
15
16
17
18
19
20
21
22
23
24
25

Mechanistic Understanding of Competitive Destabilization of Carbamazepine Cocrystals under Solvent Free Conditions

26
27
28
29
30
31
32
33
34
35
36
37
38
39
40
41
42
43
44
45
46
47
48
49
50
51
52
53
54
55
56
57
58
59
60

*M. Bashir Alsirawan,^a Xiaojun Lai,^b Rafel Prohens,^c Venu R. Vangala,^a Petroc Shelley,^d Thomas Bannan,^e David Topping,^{d,e} and Anant Paradkar^{*a}*

a. Centre for Pharmaceutical Engineering Science, University of Bradford, Bradford, D7 1DP, United Kingdom.

b. School of Chemical and Process Engineering, University of Leeds, Leeds, LS2 9JT, United Kingdom.

c. Polymorphism and Calorimetry Unit, University of Barcelona, Lluís Solé i Sabarís, 08028 Barcelona, Spain.

d. School of Earth and Environmental Sciences, University of Manchester, Manchester, M13 9PL, United Kingdom.

e. National Centre for Atmospheric Science, University of Manchester, Manchester, M13 9PL, United Kingdom.

ABSTRACT : Mechanistic understanding of competitive destabilization of carbamazepine : nicotinamide and carbamazepine : saccharin cocrystals under solvent free conditions has been

1
2
3 investigated. The crystal phase transformations were monitored using hot stage microscopy,
4
5 variable temperature powder X-ray diffraction and sublimation experiments. The destabilization
6
7 of the two cocrystals occurs via two distinct mechanisms; vapor and eutectic phase formations.
8
9
10 Vapor pressure measurements, and thermodynamic calculations using fusion and sublimation
11
12 enthalpies were in good agreement with experimental findings. The mechanistic understanding is
13
14 important to maintain stability of cocrystals during solvent free green manufacturing.
15
16

17
18 Cocrystals are increasingly attracting the interest of industries such as chemical, pharma and
19
20 agriculture for improving active component performance.¹ Researchers are working towards
21
22 development of continuous solvent free technologies such as hot melt extrusion and high shear
23
24 milling for manufacturing of cocrystals.²⁻⁴ Cocrystals display wide range of structural variations
25
26 during processing or storage including dissociation, hydration/dehydration, polymorphic
27
28 transformation, and stoichiometric changes. The reports suggest that replacement of cofomers by
29
30 structurally competitive compounds as one of the main causes responsible for cocrystal
31
32 destabilization.⁵⁻⁷ Understanding this type of destabilization is essential in multicomponent
33
34 formulations for the selection of suitable processing method, processing variables and storage
35
36 conditions. The mechanisms suggested for solvent free crystalline phase transformations involve
37
38 the formation of intermediate states with high molecular mobility.⁸ The intermediate can be vapor,
39
40 eutectic, or amorphous phase. Vapor phase is produced by molecular diffusion of materials with
41
42 relatively high vapor pressure,⁹ eutectic is formed when the mixture of reactants becomes
43
44 homogeneous and melts below melting points of pure components,¹⁰ and an amorphous solid is
45
46 formed due to brittleness of reactants.¹¹ However, there are insufficient reports discussing about
47
48 the competitive destabilization of cocrystals and no clear presentation of the mechanism thus far.⁵⁻⁷
49
50
51
52
53
54
55
56
57
58
59
60

1
2
3 The aim of current work is to develop a mechanistic explanation of cocrystal destabilization in
4 presence of competitive additives under solvent free environment.
5
6

7 Carbamazepine (CZ) forms 1:1 cocrystals with nicotinamide (NT) and saccharin (SA), which were
8 selected as competitive model systems. NT and SA are intended to compete with CZ:NT and
9 CZ:SA cocrystals, respectively. Here, we report for the first time two different pathways for
10 competitive destabilization of cocrystals in a solvent free environment. Eutectic phase mediated
11 transformation occurs during destabilization of CZ:NT in presence of SA whilst destabilization of
12 CZ:SA in presence of NT is mediated via vapor phase. The investigations were carried out using
13 variable temperature powder X-ray diffraction (VT-PXRD) and neat grinding (NG) using a ball
14 mill. Method details are provided in supporting information (SI, see section 1.2). Both techniques
15 simulate most of the solvent free processing technologies. Accordingly, we prepared mixtures
16 containing stoichiometric 1:1 molar ratios of the cocrystal and the additive, which included
17 CZ:NT+SA and CZ:SA+NT. No change was observed in PXRD patterns when CZ:NT+SA
18 mixture was subjected to heating at 120°C for 10 minutes or NG for 120 minutes. However, CZ:SA
19 formation was observed at 130 °C and complete disappearance of CZ:NT was observed at 140 °C
20 (Figure 1, left). On the other hand, heating of CZ:SA+NT at 105°C or NG for 120 minutes resulted
21 in destabilization of CZ:SA and formation of CZ:NT (Figure 1, right).
22
23
24
25
26
27
28
29
30
31
32
33
34
35
36
37
38
39
40
41
42
43
44
45
46
47
48
49
50
51
52
53
54
55
56
57
58
59
60

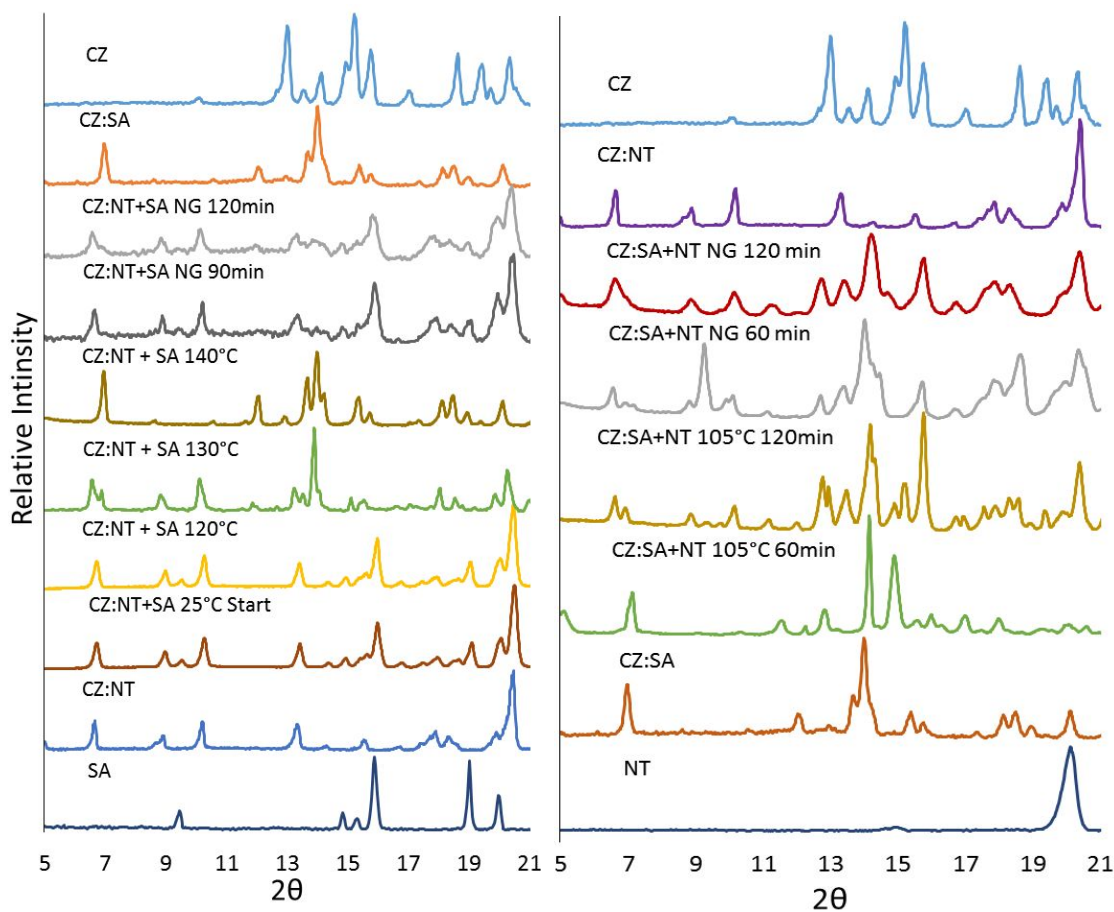


Figure 1. PXRD patterns of competitive destabilization experiments. Left: CZ:NT+SA mixture heated or subjected to neat grinding (NG) compared to experimental patterns of SA, CZ:NT, CZ:SA, and CZ. Right: CZ:SA+NT mixture heated or subjected to NG and compared to experimental patterns of NT, CZ:SA, CZ:NT, and CZ.

The individual components, their physical mixtures (PM) in 1:1 molar ratio and pure cocrystals were subjected to thermal analysis using DSC and TGA (methods are provided in SI, see sections 1.4 and 1.5). Thermal analysis data is summarized in SI, (Table S2 and Figures S3-S7). TGA data reveals that CZ:NT and CZ:SA display significant weight loss 33.4% and 27.8% at 151.8 °C and 130.8 °C, respectively. The weight loss onset temperatures are below the melting points of CZ:NT (157.2 °C) and CZ:SA (172.3°C). Similarly, pure SA exhibits weight loss at 173.2°C and below

1
2
3 its melting point (225.5 °C). This suggests that these compounds undergo sublimation. DSC
4 thermograms of CZ+NT physical mixture display two endotherms at 124.3°C which could be
5 assigned to the eutectic melting and 157.6°C assigned to CZ:NT cocrystal melting. Moreover,
6 CZ+SA PM exhibits two endotherms at 151.3°C at which a 27.3% weight loss was observed in
7 the TGA. The second endotherm is at 172.2°C assigned to CZ:SA melting. It was complex to
8 assign the first endotherm which could be a partial sublimation, eutectic or a combination of both.
9

10
11 In the previous report, 4-acetamidobenzoic acid: salicylamide cocrystal has been subjected to an
12 inert gas stream.¹² The report showed that the volatile salicylamide was carried away by the gas
13 stream while the 4-acetamidobenzoic acid with lower vapor pressure was crystallized back.¹²
14 Similarly, we tried to understand the sublimation pathway of CZ cocrystals. The individual
15 components, their physical mixtures, and stoichiometric mixtures of cocrystal with competitive
16 coformer were subjected to sublimation studies as described in SI (Section 1.6). The material was
17 heated in the sublimation apparatus for 24 hours to ensure equilibrium is achieved. The
18 temperature during the experiments was maintained at 105 °C which is below the eutectic point of
19 the cocrystal pair and rules out eutectic phase transformation. It was observed that CZ and both
20 coformers (SA and NT) undergo sublimation. The residues were analyzed using PXRD, while
21 sublimates were analyzed by Raman microscopy due to the limitation of small amount of sample.
22 Both sublimates and residuals displayed the same crystal form as that of starting product. In case
23 of CZ+NT PM, CZ:NT cocrystal was detected at the residue along with unreacted CZ and NT.
24 Additionally, only NT was detected in the sublimate. On the other hand, Both CZ and SA
25 sublimated from CZ+SA PM, while the residue remained unchanged. The cocrystal CZ:NT
26 displayed insignificant sublimation where traces of NT were detected.
27
28
29
30
31
32
33
34
35
36
37
38
39
40
41
42
43
44
45
46
47
48
49
50
51
52
53
54
55
56
57
58
59
60

1
2
3 However, CZ:SA exhibited a sublimate consisting of pure components CZ and SA. The residues
4 of both CZ:NT and CZ:SA remained unchanged. In case of CZ+SA+NT PM, the residue shows
5 partial formation of CZ:NT cocrystal and a remaining of unreacted CZ and SA. The residue in case
6 of CZ:SA + NT showed partial formation of CZ:NT and remaining of CZ:SA. A summary of
7 sublimation results is listed in Table 1. PXRD patterns and Raman spectra of sublimation outcome
8 can be found in SI (Figure S8).
9
10
11
12
13
14
15
16
17

18 **Table 1.** Summary of sublimation results. The residues were analyzed by PXRD, while sublimates
19 were analyzed by Raman microscopy.
20
21
22

Sample	Residue	Sublimate
CZ	CZ	CZ
NT	NT	NT
SA	SA	SA
CZ + NT	CZ + NT + CZ:NT	NT
CZ + SA	CZ + SA	CZ + SA
CZ:NT	CZ:NT	NT
CZ:SA	CZ:SA	CZ + SA
PM (CZ + SA + NT)	CZ + SA + CZ:NT	CZ + NT
CZ:SA + NT	CZ:NT + CZ:SA	CZ + NT + SA

1
2
3 Hot stage polarized microscopy was used for visual confirmation of the sublimation and eutectic
4 phase events. The cocrystals and the respective competing coformer crystals were placed on the
5 glass slide in the following two ways; first the two components were mixed together to enable
6 formation of the eutectic phase. In the second arrangement, the two components were separated to
7 ensure that there is no physical contact which avoids the chance of eutectic formation. *In-situ*
8 visualization data show that in the case of CZ:NT + SA mixture, it forms a eutectic phase, and
9 melts rapidly at 130 °C with simultaneous formation of plate shaped CZ:SA crystals. The reaction
10 was completed at 140 °C after ca. 5 minutes (SI, see Figures S9, S10 and separately uploaded
11 video). In a separate experiment, CZ:NT and SA were mounted separately without physical
12 contact. Only partial melting of CZ:NT cocrystal at 110 °C was observed and no formation of
13 CZ:SA cocrystal even after 58 minutes (SI, Figure S11 and separately uploaded video). Therefore,
14 reactants must be placed in contact to allow formation of eutectic phase and transformation to
15 CZ:SA. Furthermore, this shows that neither sublimation is taking place, nor CZ:NT + SA display
16 enough vapor pressure to trigger the transformation. This clearly indicates eutectic mediated
17 pathway is involved in competitive destabilization of CZ:NT by SA. On the other hand, the
18 reactants CZ:SA and NT showed formation of the new crystal phase CZ:NT when mixed as well
19 as under separated conditions. Transformation to CZ:NT was slower compared to the previous
20 process. The reaction started after 14-20 minutes at 97-100 °C and was completed at 100-110 °C
21 after 35-45 minutes (SI, see Figures S12, S13 and separately uploaded video).

22
23
24 All these data show that destabilization of CZ:NT+SA mixture occurs at temperatures above
25 125°C where it undergoes eutectic melting. This brings free CZ and SA to be in intimate contact
26 and allows CZ:SA recrystallization. However, destabilization of CZ:SA+NT can occur at
27 temperatures below 125 °C or using NG for prolonged periods.
28
29
30
31
32
33
34
35
36
37
38
39
40
41
42
43
44
45
46
47
48
49
50
51
52
53
54
55
56
57
58
59
60

The reaction involves formation of a vapor phase via sublimation of the mixture. This allows CZ to be available to interact with NT and form CZ:NT (Figure 2).

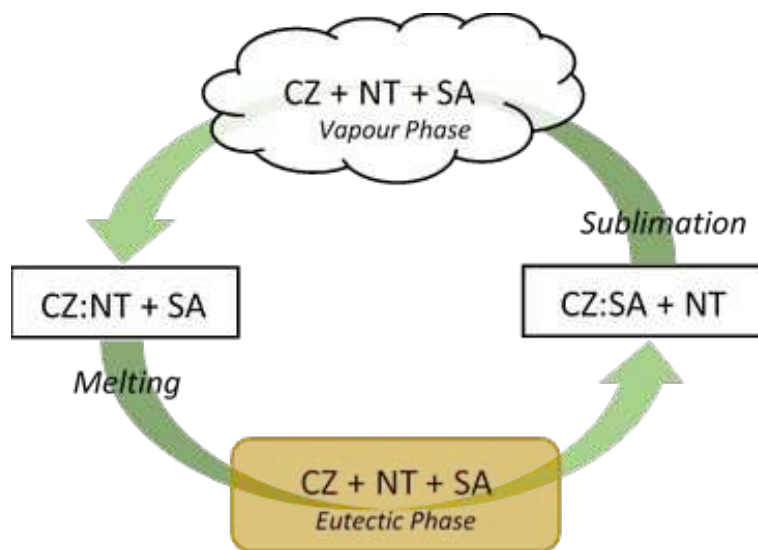
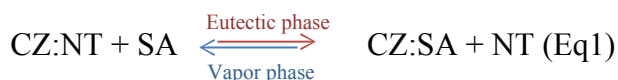


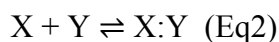
Figure 2. Proposed pathways for competitive destabilisation of CZ:SA and CZ:NT cocrystals under solvent free conditions.

To further support our proposed mechanisms, experimental results were combined with thermodynamic calculations. It provided mathematical evidence for cocrystal formation at each proposed pathway. The calculations are based on attaining high potential equilibrium state during the reaction. In current case, the equilibrium state is proposed to be either the vapor or the eutectic phase. Subsequently, the equilibrium is shifted towards the thermodynamically more stable cocrystal. Our proposed equilibrium (Equation 1) either shifts toward CZ:SA formation via eutectic phase or CZ:NT formation *via* vapor phase.



The calculations were conducted using experimental thermodynamic data. This includes fusion enthalpies (H_{fus}) and saturated vapor pressures (P). Fusion enthalpies were directly obtained from DSC profiles. However, vapor pressures of the cocrystals and their individual components were measured at a range of temperatures (298 to 328K) using Knudson Effusion Mass Spectrometry (KEMS). Then, sublimation enthalpies (H_{sub}) were calculated using Clausius-Clapeyron equation.¹³ The details of all these methods are given in the SI.

Subsequently, H_{fus} , and H_{sub} were utilized to calculate the formation stabilities of CZ:SA and CZ:NT according to (Equation 2) and assuming that entropy change in the reaction is insignificant and can be ignored¹⁴.



Where X, Y, and X:Y represents CZ, SA/NT, and CZ:SA/CZ:NT, respectively.

Next, the formation stabilities (for) were determined based on fusion enthalpy change $\Delta H_{fus-for}$ (Eq 3), and sublimation enthalpy change $\Delta H_{sub-for}$ (Eq 4).

$$\Delta H_{fus-for} = H_{fus}(X:Y) - [H_{fus}(X) + H_{fus}(Y)] \quad (\text{Eq 3})$$

$$\Delta H_{sub-for} = H_{sub}(X:Y) - [H_{sub}(X) + H_{sub}(Y)] \quad (\text{Eq 4})$$

All experimental values and related formation stabilities are summarized in Table 2. $\Delta H_{fus-for}$ values can suggest that CZ:SA (-23.4 kJ/mol) is more stable than CZ:NT (-11.5 kJ/mol). The difference in enthalpy between solid and liquid for CZ:SA ($\Delta H_{fus-for}$) is smaller than that for CZ:NT. This indicates that CZ:NT is more prone to transform to liquid state (eutectic melting) while CZ:SA structure is maintained stable at solid state. However, $\Delta H_{sub-for}$ indicates that CZ:NT (-61.97 kJ/mol) is more stable than CZ:SA (-58.06 kJ/mol). The difference in enthalpy between the solid and vapor phase ($\Delta H_{sub-for}$) is smaller in case of CZ:NT compared to CZ:SA. Therefore,

CZ:SA is more prone to sublimation while CZ:NT maintains stable at solid state. The experimental error for sublimation enthalpies measured by KEMS is found to range between 4 – 30 % of enthalpy values. Although the error is relatively high, its impact is insignificant, and the calculations still show that CZ:NT is more stable than CZ:SA.

Table 2. Fusion (H_{fus}), and sublimation enthalpies (H_{sub}) of CZ cocrystals and their components and related theoretical stabilities of cocrystal formation: $\Delta H_{\text{fus-for}}$ and $\Delta H_{\text{sub-for}}$:

Compound	H_{fus} kJ/mol	$\Delta H_{\text{fus-for}}$	H_{sub} kJ/mol	$\Delta H_{\text{sub-for}}$
CZ	24.8		74.36	
NT	11.7		62.45	
SA	25.1		37.71	
CZ:NT	25.0	-11.5	74.84	-61.97
CZ:SA	26.4	-23.4	54.01	-58.06

To further support cocrystal stabilities based on formation enthalpies, calculations were applied on destabilization process (Equation 1) to obtain a theoretical stability of cocrystal in presence of competitive coformer. The mathematical outcomes are referred to here as destabilization values (des). These were obtained using the following equations: fusion enthalpy change ($\Delta H_{\text{fus-des}}$) (Eq 5), and sublimation enthalpy change ($\Delta H_{\text{sub-des}}$) (Eq 6). A negative destabilization value indicates that the equilibrium is thermodynamically driven toward CZ:SA formation, whereas positive value indicates equilibrium shifted to CZ:NT formation.

$$\Delta H_{fus-des} = [H_{fus}(CZ:SA) + H_{fus}(NT)] - [H_{fus}(CZ:NT) + H_{fus}(SA)] \text{ (Eq 5)}$$

$$\Delta H_{sub-des} = [H_{sub}(CZ:SA) + H_{sub}(NT)] - [H_{sub}(CZ:NT) + H_{sub}(SA)] \text{ (Eq 6)}$$

Additionally, destabilization related Gibbs free energy change was calculated using vapor pressure (P) measurements (Eq 7) at seven temperature points in the range of 298 – 328 K.

$$\Delta G_{sub-des} = -RT \ln \frac{P_{CZ:NT} P_{SA}}{P_{CZ:SA} P_{NT}} \text{ (Eq 7)}$$

The destabilization value related to enthalpy of fusion $\Delta H_{fus-des}$ (-12.0 kJ/mol) indicates that equilibrium favors CZ:SA formation.

Table 3. Destabilization related fusion enthalpy change ($\Delta H_{fus-des}$), and sublimation enthalpy change ($\Delta H_{sub-des}$) of (Eq 1) linked to observed cocrystal produced via neat grinding (NG) and heat and suggested pathway.

$\Delta H_{fus-des}$	$\Delta H_{sub-des}$	Process	Observed	Pathway
-12.0 kJ/mol	3.91 kJ/mol	NG 120 min	CZ:NT	Vapor
		Heat 105°C		
		Heat 140°C	CZ:SA	Eutectic

The association of eutectic phase route during CZ:SA formation is highly supported by ΔH_{fus} . Fusion enthalpies are robust thermodynamic representation of melt/eutectic formation. They reflect the energy required for melting/solidification, hence, the cohesiveness of a solid.^{15–17} This suggests that competitive destabilization of CZ:NT + SA occurs via the formation of an intermediate eutectic liquid phase of CZ+NT+SA mixture. In this environment, the CZ-SA

interaction is stronger than the CZ-NT interaction, which results in nucleation and subsequent crystal growth of the CZ:SA cocrystal.

On the other hand, destabilization values related to sublimation enthalpy $\Delta H_{\text{sub-des}}$ (3.91 kJ/mol) (Table 3) and Gibbs free energy of sublimation $\Delta G_{\text{sub-des}}$ produced positive values (Table 4) suggesting that equilibrium favors CZ:NT formation.

Table 4. Destabilization related Gibbs free energy change of sublimation, using vapor pressure values (P) measured at temperature range of 298 – 328 K.

T(K)	$\Delta G_{\text{sub-des}}$ (J/mol)	P_{NT} (mPa)	P_{SA} (mPa)	$P_{\text{CZ:NT}}$ (mPa)	$P_{\text{CZ:SA}}$ (mPa)
298	380.50	2.01	4.98	0.88	0.31
303	349.97	3.05	6.40	1.20	0.50
308	916.24	4.56	8.16	1.64	0.64
313	1676.41	6.73	10.33	2.36	0.81
318	1242.06	9.81	12.97	3.30	1.56
323	621.29	14.14	16.18	4.47	3.10
328	711.90	20.16	20.04	6.48	5.02

Sublimation related stabilities indicate vapor phase pathway is involved in the formation of CZ:NT. This suggests that CZ:SA + NT reaches an intermediate vapor phase having a vapor pressure that overcomes the vapor pressure of pure CZ:NT. This leads to a supersaturation state with respect to CZ:NT which triggers the nucleation and subsequent crystal growth of CZ:NT cocrystal. The predictability of calculated theoretical stabilities was in good agreement to experimental findings (Figure 3).

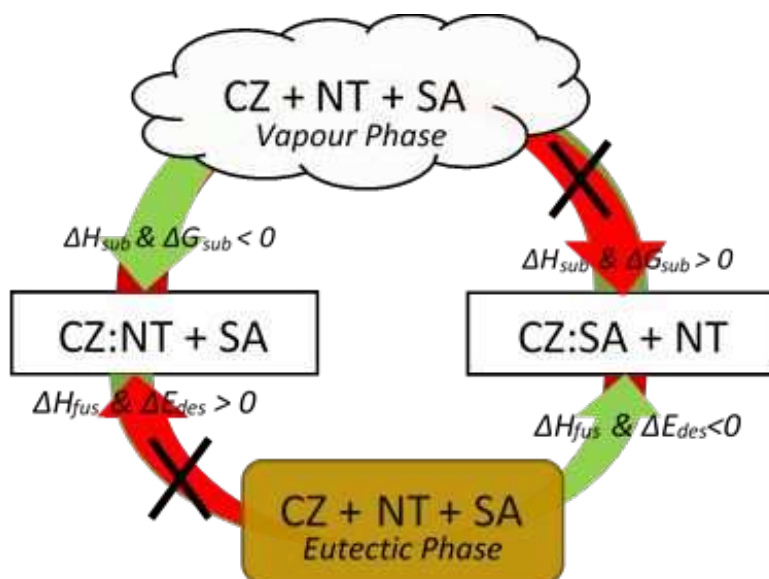


Figure 3. A correlation between calculated thermodynamic values and experimental destabilizations of CZ:NT and CZ:SA cocrystals mediated by eutectic and vapor phase formation, respectively.

CONCLUSION:

CZ:NT is destabilized in presence of SA at 120 °C – 140 °C temperature range, which is close to the CZ+NT eutectic and CZ:NT melting temperature range. The formation of a melt phase was observed both in the sublimation apparatus and under hot-stage microscopy. On the other hand, no reaction was observed when CZ:NT and SA were placed together without being in contact and heated up to 140 °C under microscopy as well as during the NG of CZ:NT+SA. The theoretical stabilities related to fusion enthalpies demonstrated a preferred formation of CZ:SA over CZ:NT. This confirms eutectic phase pathway during competitive destabilization of CZ:NT in presence of SA and formation of CZ:SA. On the other hand, during NG or heating below 120 °C where eutectic formation is avoided, CZ:SA cocrystal is destabilized in presence of NT. Sublimation experiments show that CZ:SA is more prone to sublimation than CZ:NT. Moreover, CZ:NT cocrystal is formed after maintaining CZ+NT, CZ+NT+SA, and CZ:SA+NT mixtures at 105 °C. Additionally, CZ:NT

1
2
3 formation could be visualized under hot stage microscopy when CZ:SA and NT were placed in
4 contact or separated without formation of eutectic phase. Moreover, theoretical stability values
5 related to enthalpy and Gibbs free energy of sublimation suggests that CZ:NT formation is
6 preferred. These findings support the involvement of Vapor phase pathway during competitive
7 destabilization of CZ:SA + NT and formation of CZ:NT. This is the first report with focus on
8 competitive destabilization of cocrystal by a cofomer during green synthesis of cocrystals. Each
9 condition conveys specific mechanism which result in a unique thermodynamic outcome.
10 Understanding of such competitive mechanisms can lead to better process design and improving
11 the control of produced cocrystals.
12
13
14
15
16
17
18
19
20
21
22
23

24 **Corresponding Author**

25
26
27 Anant Paradkar, a.paradkar1@bradford.ac.uk. Centre for Pharmaceutical Engineering Science,
28 University of Bradford, Bradford, D7 1DP, United Kingdom.
29
30
31

32 **Author Contributions**

33
34
35 The manuscript was written through contributions of all authors. All authors have given approval
36 to the final version of the manuscript.
37
38
39

40 **ACKNOWLEDGMENT**

41
42
43 Authors would like to thank EPSRC (EP/J003360/1, EP/L027011/1). M. Bashir would like to
44 thank CARA for providing doctoral degree scholarship.
45
46
47

48 **REFERENCES**

- 49
50
51 (1) Karimi-Jafari, M.; Padrela, L.; Walker, G. M.; Croker, D. M. Creating Cocrystals: A Review
52 of Pharmaceutical Cocrystal Preparation Routes and Applications. *Cryst. Growth Des.*
53 **2018**, *18*, 6370–6387. <https://doi.org/10.1021/acs.cgd.8b00933>.
54
55
56
57
58
59
60

- 1
2
3 (2) Korde, S.; Pagire, S.; Pan, H.; Seaton, C.; Kelly, A.; Chen, Y.; Wang, Q.; Coates, P.;
4 Paradkar, A. Continuous Manufacturing of Cocrystals Using Solid State Shear Milling
5 Technology. *Cryst. Growth Des.* **2018**, *18*, 2297–2304.
6
7 <https://doi.org/10.1021/acs.cgd.7b01733>.
8
9
10
11
12 (3) Rogers, L.; Jensen, K. F. Continuous Manufacturing – the Green Chemistry Promise? *Green*
13 *Chem.* **2019**, *21*, 3481–3498. <https://doi.org/10.1039/C9GC00773C>.
14
15
16
17 (4) Cue, B. W.; Zhang, J. Green Process Chemistry in the Pharmaceutical Industry. *Green*
18 *Chem. Lett. Rev.* **2009**, *2*, 193–211. <https://doi.org/10.1080/17518250903258150>.
19
20
21
22 (5) Alsirawan, M. B. B.; Vangala, V. R. V. R.; Kendrick, J.; Leusen, F. J. F. J. J.; Paradkar, A.
23
24 Cofomer Replacement as an Indicator for Thermodynamic Instability of Cocrystals:
25 Competitive Transformation of Caffeine:Dicarboxylic Acid. *Cryst. Growth Des.* **2016**, *16*,
26 3072–3075. <https://doi.org/10.1021/acs.cgd.6b00458>.
27
28
29
30
31 (6) Fischer, F.; Lubjuhn, D.; Greiser, S.; Rademann, K.; Emmerling, F. Supply and Demand in
32 the Ball Mill: Competitive Cocrystal Reactions. *Cryst. Growth Des.* **2016**, *16*, 5843–5851.
33
34 <https://doi.org/10.1021/acs.cgd.6b00928>.
35
36
37
38 (7) Suzuki, N.; Kawahata, M.; Yamaguchi, K.; Suzuki, T.; Tomono, K.; Fukami, T.
39
40 Comparison of the Relative Stability of Pharmaceutical Cocrystals Consisting of
41 Paracetamol and Dicarboxylic Acids. *Drug Dev. Ind. Pharm.* **2018**, *44*, 582–589.
42
43 <https://doi.org/10.1080/03639045.2017.1405433>.
44
45
46
47 (8) Friščić, T.; Jones, W. Recent Advances in Understanding the Mechanism of Cocrystal
48 Formation via Grinding. *Cryst. Growth Des.* **2009**, *9*, 1621–1637.
49
50 <https://doi.org/10.1021/cg800764n>.
51
52
53
54 (9) Kuroda, R.; Imai, Y.; Tajima, N. Generation of a Co-Crystal Phase with Novel Coloristic
55
56
57
58
59
60

- 1
2
3 Properties via Solid State Grinding Procedures. *Chem. Commun.* **2002**, No. 23, 2848–2849.
4
5 <https://doi.org/10.1039/b207417f>.
6
7
8 (10) Chadwick, K.; Davey, R.; Cross, W. How Does Grinding Produce Co-Crystals? Insights
9
10 from the Case of Benzophenone and Diphenylamine. *CrystEngComm* **2007**, *9*, 732.
11
12 <https://doi.org/10.1039/b709411f>.
13
14
15 (11) Nguyen, K. L.; Frisci , T.; Day, G. M.; Gladden, L. F.; Jones, W. Terahertz Time-Domain
16
17 Spectroscopy and the Quantitative Monitoring of Mechanochemical Cocrystal Formation.
18
19 *Nat. Mater.* **2007**, *6*, 206–209. <https://doi.org/10.1038/nmat1848>.
20
21
22 (12) Manin, A. N.; Voronin, A. P.; Manin, N. G.; Vener, M. V.; Shishkina, A. V.; Lermontov,
23
24 A. S.; Perlovich, G. L. Salicylamide Cocrystals: Screening, Crystal Structure, Sublimation
25
26 Thermodynamics, Dissolution, and Solid-State DFT Calculations. *J. Phys. Chem. B* **2014**,
27
28 *118*, 6803–6814. <https://doi.org/10.1021/jp5032898>.
29
30
31 (13) Booth, A. M.; Markus, T.; Mcfiggans, G.; Percival, C. J.; McGillen, M. R.; Topping, D. O.
32
33 Design and Construction of a Simple Knudsen Effusion Mass Spectrometer (KEMS)
34
35 System for Vapour Pressure Measurements of Low Volatility Organics. *Atmos. Meas. Tech*
36
37 **2009**, *2*, 355–361. <https://doi.org/10.5194/amt-2-355-2009>.
38
39
40 (14) Verwer, P.; Leusen, F. J. J. Computer Simulation to Predict Possible Crystal Polymorphs.
41
42 In *Reviews in Computational Chemistry*; John Wiley & Sons, Inc., 2007; pp 327–365.
43
44 <https://doi.org/10.1002/9780470125892.ch7>.
45
46
47 (15) Issa, N.; Karamertzanis, P. G.; Welch, G. W. A.; Price, S. L. Can the Formation of
48
49 Pharmaceutical Cocrystals Be Computationally Predicted? I. Comparison of Lattice
50
51 Energies. *Cryst. Growth Des.* **2009**, *9*, 442–453. <https://doi.org/10.1021/cg800685z>.
52
53
54 (16) Oliveira, M. A.; Peterson, M. L.; Davey, R. J. Relative Enthalpy of Formation for Co-
55
56
57
58
59
60

1
2
3 Crystals of Small Organic Molecules. *Cryst. Growth Des.* **2011**, *11*, 449–457.
4
5 <https://doi.org/10.1021/cg101214m>.
6

- 7
8 (17) Galindo-García, U.; Torres, L. A. Crystal Structure at the Origin of the Thermal Stability
9
10 and Large Enthalpy of Fusion and Sublimation Values of Calixarenes. *Cryst. Growth Des.*
11
12 **2020**, *20*, 1302–1310. <https://doi.org/10.1021/acs.cgd.9b01562>.
13
14
15
16
17
18
19
20
21
22
23
24
25
26
27
28
29
30
31
32
33
34
35
36
37
38
39
40
41
42
43
44
45
46
47
48
49
50
51
52
53
54
55
56
57
58
59
60